ISSN: 2633-4828 Vol. 5 No.4, December, 2023

International Journal of Applied Engineering & Technology

EXPERIMENTAL INVESTIGATION ON FLUID FLOW BEHAVIOR AND CONVECTIVE HEAT TRANSFER PERFORMANCE OF WATER, ETHYLENE GLYCOL-BASED ZINC OXIDE NANOFLUID IN AIR FINNED CROSS FLOW HEAT EXCHANGER

Nitin Mahay[1] and Raj Kumar Yadav[2]
[1]Ph.D Research Scholar and [2]Professor, Mechanical Engineering Department, SLIET, Longowal, Punjab, India
[1]Nitinmahay@gmail.com and [2] Rkyd@sliet.ac.in

ABSTRACT
In the current study, overall heat transfer coefficient of water and ethylene glycol (60DW:40EG) based Zinc oxide nanoparticles in a cross-flow heat exchanger has been evaluated under the laminar flow regime. The effect of concentration in the range of 0.25, 0.5 and 1.0 vol.% of stabilized ZnO/ (60DW:40EG) nanofluid have been measured with variation in flow rate in the segment of 12-15 LPM. The air-cooled cross-flow heat exchanger consisted of 2 rows of vertical aluminum tubes and each row contained 76 tubes. Multi-louvered fins are inaugurated on the outer surface of the tubes and air with different velocities (3.16, 4.26,5.33 and 6.22 m/s) is allowed to pass through them. In addition, the hot working fluid is permitted to enter into the radiator at different temperatures viz. 50, 60 and 70°C. The result demonstrates that the water side Nusselt number gets enhanced by 4.262% and 11.92% with the increase in Reynolds number at 0.25 and 0.5 vol.% concentration respectively. The friction factor is enhanced by 52.631%, 26.315% and 15.789% for 1.0%, 0.5% and 0.25% nanofluid concentration respectively. However, drops in friction factor by 35.578% at 0.25, 38.636% at 0.5 and 29.916 % at 1.0 vol% have been observed when the Reynolds number increases from 144 to 180. On the air side maximum improvement in Nusselt number by 51.91% with 1.0% vol. concentration of nanofluid is observed and that of Colburn factor of air gets enhanced by 16.439%, 24.657% and 41.096% for 0.25%, 0.5% and 1.0% concentration of nanofluid. The effectiveness of the heat exchanger shows a significant rise to 75.29% with 1.0% vol. nanofluid concentration whereas that is 68.05% using base fluid.

Keywords: Zinc Oxide Nanofluid, Thermo-physical Properties Radiator, Overall Heat Transfer Coefficient, Laminar Flow Regime, Heat Transfer Rate.

TABLE OF SYMBOLS

Notations	Particulars	Unit
A_t	Total heat transfer surface area	m^2
A_t	Total heat transfer surface area	m^2
A_0	Free flow areas of the exchanger	m^2
A_f	Free flow area of fin exposed to heat transfer	m^2
A_{fr}	Air side frontal area of the exchanger	m^2
$A_{c,t}$	Cross-sectional area of tube	m^2
A_w	Air ways	-
T_t	Tube thickness	m
T_w	Tube width	m
T_l	Total length	m
$T_{t,l}$	Total tube length in core dimension,	m
T_s	Tube sheet thickness	m
F_t	Fin thickness	m
F_l	Fin length	m
F_w	Fin width	m
N_t	Number of tubes one side	-
N_f	Number of fins in between two tubes	-

A	Tube spacing	m
B	Fin spacing	m
W	Fluid flow (air) length,	m
C_p	Specific heat of fluid at constant pressure,	J/kg C
D_h	Hydraulic diameter	m
f	Friction factor	Dimensionless
G	Mass velocity,	Kg/ m^2 s
C	Heat capacity rate h Heat transfer coefficient	W/ m^2 C
J	Colburn factor	Dimensionless
K	Fluid thermal conductivity	W/m C
K_f	Thermal conductivity of fin materials	W/m C.
LPH	Liters per hour	-
P	Pressure	Pa
Pr	Prandtl number	Dimensionless
Nu	Nusselt number	Dimensionless
U	Overall heat transfer coefficient	W/ m^2 C
V	Volume	m^3
v	Velocity	m/s
m	Fluid mass flow rate	kg/s
α	Ratio of total heat transfer area of one side to its volume	m^2 / m^3
ρ	Density	kg/ m^3
ϕ	Diameter	m
ε	Heat exchanger effectiveness	-
η_f	Fin efficiency	-
η_0	Overall efficiency	-

SUBSCRIPTS

Notations	Particulars
A	Air
B	Bulk
C	Cold fluid side
H	Hot fluid side
W	Water
1	Inlet conditions
2	Outlet conditions

INTRODUCTION

In the modern era of technological advancement, high price of energy attracts the consideration of researchers to apply some energy-saving techniques as much as possible. For the energy rejection or recovery heat exchangers play a pivotal role and have become a major component in numerous industries such as nuclear power plants, chemical industries, automobile industries and microelectron mechanical systems (MEMS) [1]. The overall efficiency of the systems depends on the circulating fluids that are an integral part of the heat exchanger. However, lower thermal conductivity and poor properties of conventional fluids become a barrier in optimizing the full efficiency of the devices. Different techniques have been made to enhance the heat transfer rate, reduction in size of heat exchanger and hence enhancement in efficiency of heat transfer components [2]. These techniques consist of active techniques and passive techniques such as surface vibration, fluid stirring and geometry modification. The thermal conductivity of the metal or metal oxide is always higher than that of liquid and gases. The addition of solid particles into the fluids plays a major role in enhancing the thermal conductivity of the resultant fluids. In spite of all the addition of particles increases the thermal conductivity of the fluids but simultaneously they have the potential to cause some problems such as sedimentation of the particles into the fluid and clogging of flow channels. Sensing this need "Choi" dispersed the nano-size particles into base fluid and concluded that the addition of solid particles into fluid increases the thermal conductivity of resultant fluid and hence gave birth to a new term "nanofluids" [3]. Several studies have been conducted by different researchers on the convective heat transfer coefficient and overall heat transfer of the heat exchanger with the aid of nanofluids and compared it with conventional fluids such as water, ethylene glycol, or a mixture of both at different ratios. The experimental studies conducted by different researchers show improved thermal conductivity and enhancement in convective heat transfer thus increase in overall heat transfer rate along with a slight increase in the pressure drop results in a little more pumping power requirement [4-6].

Leyong et al. [7] reported that about 3.8 % of heat transfer can be intensified with the addition of 2% of copper nanoparticles into the base fluid when the Reynold numbers are 5000 for coolant and 6000 for the air. In addition to this, with the aid of 2% copper nanofluids, a reduction of 18.7% in the frontal area of the radiator as compared to the initial configuration without affecting the heat transfer characteristics has been investigated.

Kalantri D et. al. [8] investigated the effect of $CuFe_2O_4$/ Water (average diameter 28nm) nanofluid with different volumetric concentrations of nanoparticles in the fluid over a cross-flow heat exchanger under the turbulent flow conditions with a motive to enhance the heat transfer rate and evaluate that the overall heat transfer coefficient and Maximum Performance criterion raised by 92.3% and 44.46% when to compare with base fluid. In another study (2020) Kumar A. et. al [9] performed a comprehensive and comparative study for a better understanding of the effect of three different oxide-based nanoparticles i.e. Aluminium, copper and zinc in a mixture of water and ethylene glycol with 60 and 40 percent respectively. The actual size louvered fin car radiator was considered as a heat exchanger. Thermophysical properties such as viscosity and heat transfer characteristics have been evaluated and reported that the heat transfer coefficient is enhanced by 42.5% with Aluminium oxide, 47.4% by zinc oxide and 51.1% by copper oxide with additions of 2% volumetric concentration of nanoparticles in each nanofluids. The study made clear that the copper oxide nanoparticles-based nanofluids show the most effectiveness among the other nanofluids.

XIaoke li et. al. [10] fabricated the ethylene glycol-based nano-coolant of silicon carbide (SiC) and multi-wall carbon nanotubes (MWCNT) for a car radiator to investigate the comparative study between the nanofluid and conventional fluid. Additions of 0.4% volumetric concentration into the base fluid raise the thermal conductivity of the overall fluid by 32.01% which is further increased with the increase in concentration of the particles in the base fluid. However, the viscosity of the nanofluid also increased but declined with an increase in temperature. 26% enhancement has been recorded in convective heat transfer coefficient when comparing the nano-coolant with base fluid (EG) under the same parametric conditions.

Hafeez B.M. et.al. [11] carried out experimental research to find out the heat transfer characteristics of Aluminium Oxide (Al_2O_3), copper oxide (CuO) and titanium oxide (TiO_2) based nanofluids by governing the automobile radiator as a heat exchanger while slip conditions were talking into account and found an inversely proportional relation between the Grashof Number and thermal performance of the radiator. The study concluded that the temperature of the nanofluid was affected by the thermal slip effect and titanium oxide-based nanofluids ranked at the topmost position. However, CuO nanofluids fall to the last position for the same. For thermal performance, Aluminium oxide (Al_2O_3) based nanofluid was awarded as the best nanofluid among the three nanofluids.

Kalantari D. et al. [12] attempted to enhance the efficiency of a cross-flow heat exchanger by replacing the traditional coolant with a water-based $CuFe_2O_4$ nanofluid under turbulent flow conditions. The volumetric concentration of the particles into the base fluid varied from 0 to 0.9 % whereas the inlet temperature and fan speed fell in the range of 72-88 and 1500-2500 respectively. The result shows that the universal heat transfer coefficient raised by 92.3% at an inlet temperature of $72^{O}C$, 0.1% volumetric concentration of the particles into the fluid and low fan speed (1500RPM) when compared to the base fluid. However, a 44.46% hike has been noticed in the maximum Performance Evaluation Criterion (PEC). An equal proportion of water and ethylene glycol-based nanofluids are prepared by dispersing the particles of Aluminium oxide and titanium oxide by Said Zafar et.al. [13] for enhancing the performance of an automobile radiator. Considerable attention is paid towards the thermo-physical properties of the nanofluid. Experimental investigations show that the thermal performance gets significantly hiked by 24.21% by using Aluminium oxide nanofluid at a concentration of 0.3%. In addition, the value of PEC lies in the range of 1.03 -1.31.

The present experimental work has been carried out to understand heat transfer characteristics of highly diluted water-ethylene glycol-based Zinc Oxide nanofluids in actual-size automobile radiator under laminar flow conditions. The selected range of input parameters such as flow rate of coolant, inlet temperature of coolant and velocity of cooling media is based on the real working condition of an automobile engine where heat exchanger is employed and which appears as an unattended area in literature. In addition to this, rheological properties of nanofluids like thermal conductivity, density and viscosity of synthesized nanofluids have been evaluated at different temperatures and varying concentrations of nanoparticles in the base fluid.

EXPERIMENTAL SETUP AND DETAIL DESCRIPTION

Fig.1 represents the outlook of the experimental setup used for the current study. Also, the schematic diagram indicating different flow channels is shown in Fig.2. The organized experimental setup consists of the following components:

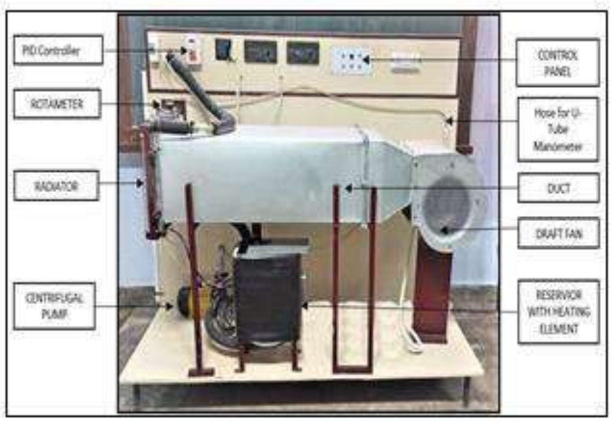

Fig. 1: Experimental Setup Test Rig.

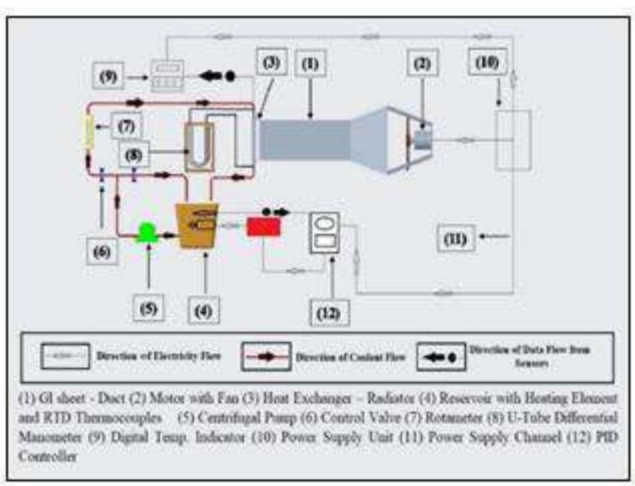

Fig. 2: The Schematic of Experimental Setup.

Reservoir: The reservoir is made up of 12-gauge GI sheets and the maximum capacity of the tank is about 12.5 liters. The upper ¾ part of the tank is rectangular while the rest part (base) is semi-hexagonal in shape. 3 heating elements (3 KW each) are placed inside the reservoir to escalate the temperature of the cooling fluid equivalent to the engine temperature considered at about 80^0 C [14]. A PID controller-operated RTD thermocouple is allowed to hang at the center of the reservoir to maintain the temperature of the coolant.

Centrifugal Pump: A centrifugal pump of 0.5 HP having Q_{max}= 35L/min, H_{max}=30m and 3000 RPM is installed to circulate the cooling fluid from reservoir to the heat exchanger (Radiator). The suction hose of the pump is attached at the bottom of the reservoir while the discharging hose is connected with the heat exchanger through a bypass valve.

Rotameter with By-pass Valve: A rotameter (range 5 LPM - 40 LPM) is used to regulate the discharge to the radiator and is applied between the bypass valve and the heat exchanger. By-pass valves consist of one inlet section and two outlet ports and two regulating valves. One outlet port is attached to the rotameter and a second port is attached to the reservoir. Regulating valves are operating manually to maintain the flow rate which can be directly observed from the rotameter.

Controller Unit: The controller unit consists of various switches such as one-way switch: to operate a digital temperature indicator, a regulator: to maintain the fan speed i.e. velocity of air, PID controller with a relay: to maintain the temperature of the fluid within the reservoir.

U-Tube Differential Manometer: A mercury-operated U-tube differential Manometer is attached at the water side inlet and outlet chamber of the radiator to measure the pressure drop within the radiator tubes. However, the limbs of water water-operated U-tube manometer are connected at the air inlet and air outlet side of the radiator for analyzing the friction factor within the extended surfaces i.e. fins of the radiator.

Duct with Fan and Heat Exchanger: The duct (length=0.25m convergent and 0.75m rectangular), furnished with a 20-gauge GI sheet is initiated into the experimental setup. One end of the duct consists of a fan (app. 3800rpm) while the other end consists of a radiator. The speed of the fan can be varied through a regulator provided in the control panel.

RTD Pt-100 Thermocouples: RTD Pt-100 thermocouples are installed at different locations on the inlet and outlet section of the radiator (both air and water side). These thermocouples are well connected with an electricity-operated Digital Temperature Indicator (DTI). The function of DTI is to convert the signals being transferred by the thermocouples and display them in terms of Degree Celsius.

Heat Exchanger: The heat exchanger (louvered fin radiator) used in the current study belongs to the vehicle having approx. 1500cc engine load. The configuration of the heat exchanger is shown in Table 1. A mercury-operated U-Tube differential manometer is attached to inlet and outlet limbs of the radiator to measure pressure drops during the cycle within the radiator.

Table 1: Configuration of Heat Exchanger

Configuration	Category
Number of passes	1
Number of rows	2
Profile of tubes	Rectangular with half-circular end
Material of tubes and fin	Aluminium
Profile of fins	Multi-louvered fins
Dimension of radiator: Core Height x Core Length x Core Width	(33.3 X 49 X 3.5) cm
Number of fins per tube	103

ISSN: 2633-4828 Vol. 5 No.4, December, 2023

PREPARATION OF ZINC OXIDE NANOFLUIDS

In the current study, Zinc oxide (ZnO) having an average particle size of 43 nm is dispersed into the mixture of water and ethylene glycol (60 Distilled water: 40 Ethylene Glycol) to form a colloidal mixture thus called nanofluids shown in Fig 3. Further, a small amount of Sodium Dodecyl Sulfate (SDS) acts as a dispersant and is added into the fluids for better stability. It is noticeable that sedimentation start occurring on the 18^{th} day and can be observed visually in sample (B) that prepared without surfactant. However, nanoparticles in the sample (A) are still uniformly suspended.

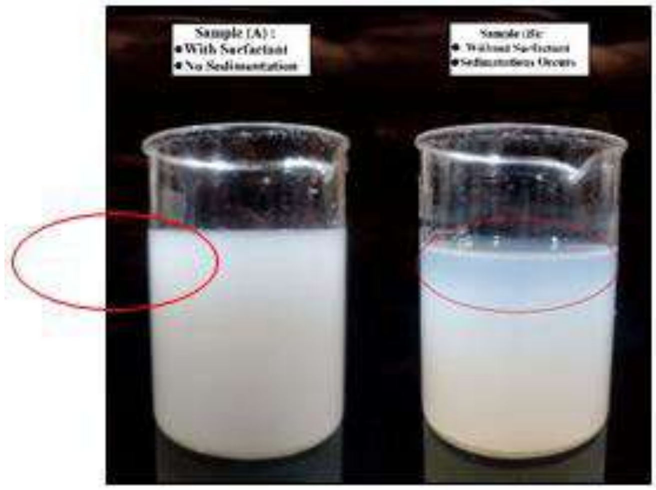

Fig. 3: Prepared Sample of ZnO Nanoparticles

The physical properties of the Zinc Oxide nanoparticles are listed in Table 2 below. The SEM (Scanning Electron Microscopy) and XRD (X-ray diffraction) images are shown in Fig. 4 and Fig. 5 respectively. Three kinds of approaches are available [15] for the synthesis of nanofluids. These approaches consist of (1) Converting the pH value of the suspension (2) Additions of surface activator into the fluid (3) putting the fluid into an ultrasonicator. For the present study, an ultrasonicator is used to prepare the nanofluid.

Table 2: Physical Properties of ZnO Nanoparticles

Particulars	Configuration
Chemical Name	ZnO - nanoparticles
Morphology of Particles	Spherical
Appearance	Milky White power
Average Particle Size, Purity	43 nm, > 99.9%
Density	5500kg/m^3
Thermal Conductivity	50W/m K (at room temp.)

To commence with, the desired amount of nanoparticles are added into the base fluid to form a colloidal suspension and thus, to form a homogeneous mixture and then put the resultant suspension into the bath tank of the sonicator (Model: BRANSON) filled with water. The working frequency is set at 24kHz and the useful power output of 800W. After the 2 hours of sonication, the uniform dispersion of nanoparticles can be observed by the visual inspection. Few samples from the nanofluids are collected to conduct the various tests. In the present study, three different volumetric concentrations 0.25%, 0.5% and 1.0% of the nanofluids are prepared to compare the effect of concentration of the nanofluid over the heat exchanger.

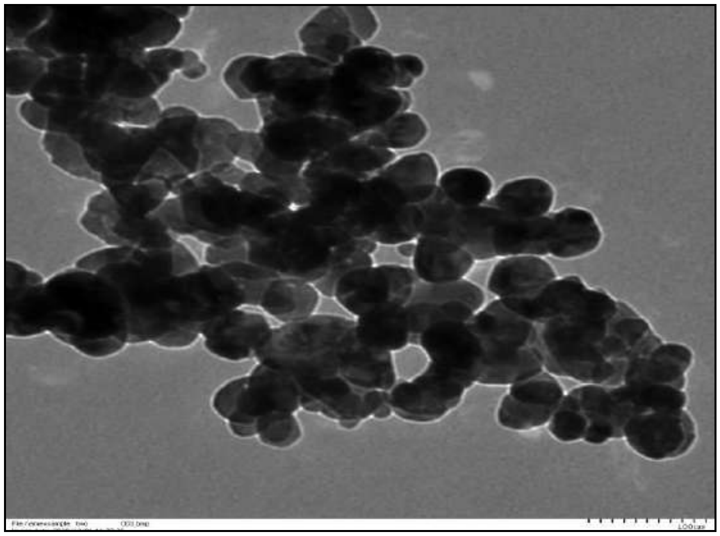

Fig. 4: SEM Photograph of ZnO Nanoparticle

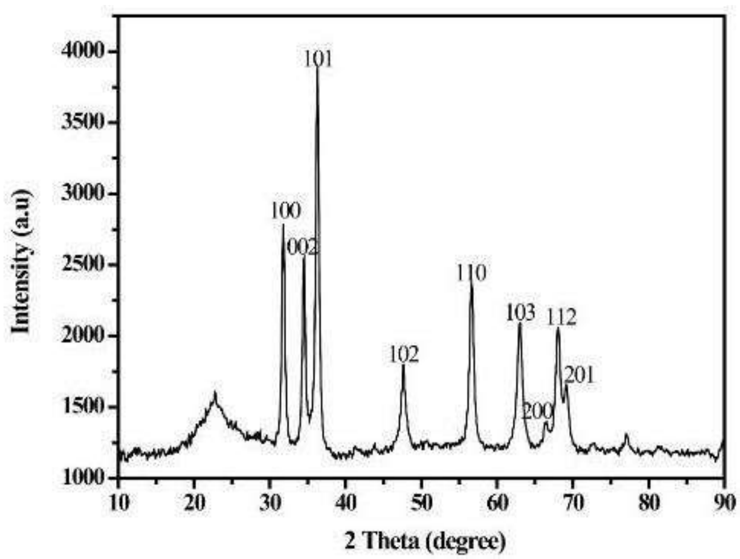

Fig. 5: XRD image of ZnO Nanoparticle

Measurement of Thermo-Physical Properties of Nanofluids:

To understand the comparative effect of nanofluids and the base coolant for car radiator, it is mandatory to measure the various thermophysical properties of the nanofluids such as thermal conductivity, density, viscosity and specific heat.

KD-II Pro Thermal Analyzer

Thermal conductivity of the nanofluids is measured with KD- II Pro thermal analyzer shown in Fig.6, a hand handler type of penal consisting of a display and a movable needle sensor. The needle sensor is dipped into the medium through which the conductivity is measured. The detailed specification of the thermal analyzer is shown in Table 3. Two different kinds of needles (sensors) can be attached to the penal. Single needle sensor, to measure the thermal conductivity and resistivity while dual needle sensors are applicable for measuring the specific heat and thermal diffusivity.

ISSN: 2633-4828 Vol. 5 No.4, December, 2023

Fig. 6: KD-II Pro Thermal Analyzer.

Table 3: Detailed Specification of KD-II Pro Thermal Analyzer

Particulars	Configuration
Size of the case (L X W X H)	15.5 cm X 9.5 cm X 3.5 cm
Reading mode	Manual and automatic read
Display size	3cm X 6cm,128 X 64-pix. LCD
Operating Power	4 AA battery connected in series
Storage capacity	4095 measurement in memory (available for download)
Operating temperature	10^{O}C to 80^{O}C

The thermal conductivity of zinc oxide-based nanofluids is measured at three different concentrations and temperature ranges. The samples of the nanofluid at a specific concentration are collected into the glass tube sample holder. The cap of the sample holder is provided with a small hole through which the needle sensor is inserted into the fluid. The value of thermal conductivity is directly indicated on the panel's display.

Pycnometer or Specific Gravity Bottle:

In the current study, a pycnometer is used to measure the specific gravity of nanofluid. As shown in Fig. 7, a pycnometer consists of a bottle of specific volume with a close-fitted cap over it. A small capillary is provided into the cap. At a certain temperature, a gravity bottle holds a specific volume of fluid and extra fluids released through the capillary. The difference in weight (filled gravity bottle – empty gravity bottle) is measured. The net weight is divided by the weight of distilled water of equal volume resulting in the specific gravity of the given sample.

Fig. 7: Pycnometer or Specific Gravity Bottle

Brookfield DV-I+ Viscometer: `

The viscosity of the nanofluids is measured from the Brookfield DV-1 viscometer. Viscosity is the measurement of drag forces that occur during the flow. It gives fluid parameters like shear stress and viscosity at a given shear rate [16-18]. The principle behind the working of an instrument is the measurement of the deflection of a calibrated spring through the rotary transducer. On another end, a rotary spindle is attached to the spring, as it comes in contact with the fluid of which viscosity is to be measured, the viscous forces resist the spindle from rotating which further causes a small deflection into the spring which directly recorded in terms of centipoise. Fig. 8 represents the detailed working of Brookfield DV-1 and specifications of instruments are given in Table 4.

Fig. 8: Brookfield DV-I+ Rheometer for Viscosity Measurement

Table 4: Detailed Specification of DV-I + Viscometer

Specification	Detail
Model Name	DV-I+ viscometer
Operating Environmental Temp.:	0°C to 40°C
Accuracy	± 1.0% Full-Scale Range
Viscosity Repeatability	± 0.2% of Full-Scale Range
Temperature Sensing Range	-100°C to +300°C
Accuracy:	± 1°C: -100°C to +149°C ± 2°C: +150°C to +300°C

EXPERIMENTAL WORK AND CALCULATIONS

For the present study, the louvered fin and flat tube radiator of the Mahindra 1500 CC automobile have been selected. The heat exchanger consisted of 2 rows of vertical flat tubes with semicircular ends and each row having 76 tubes. The effectiveness of the heat exchanger (radiator) is analyzed under the various input parameters such as inlet temperature of the fluid (50^{o}C, 60^{o}C and 70^{o}C), coolant flow rate (12,13,14 and 15 LPM), the concentration of the particles into the fluid (0.25%, 0.5% and 1.0% volumetric concentration) and air velocity (3.16, 4.26,5.53 and 6.22 m/s).

For the detailed performance evaluation, the analysis of heat exchanger is divided into two parts:

Tube side or water side: Heated fluid is transferred at a given temperature from the reservoir through the tubes of the radiator and collected into the bottom chamber at a certain temperature. Data is acquired with the help of thermocouples installed at different locations (3 sensors in both inlet and outlet chamber), the difference in temperatures is calculated to find the relation with the Nusselt Number and Reynolds Number. The bulk mean temperature of the fluid is evaluated by considering the mean of inlet and outlet temperatures. Thermophysical properties of coolant at a bulk mean temperature of 329.65 K are shown in table [19].

Table 5: Thermo Physical Properties of Coolant at Bulk Mean Temperature of 329.65K

Bulk mean temp.	**Thermal conductivity (k_w), W/mK**	**Density (ρ_w) kg/m^3**	**Dynamic viscosity (μ_w) Ns/m^2**	**Prandtl Number**
329.65 K	0.38785 W/mK	1042.1 kg/m^3	0.0012016 Ns/m^2	9.87

Following are the relations to find the heat transfer coefficient and friction factor [18]:

$T_{bm} = \frac{Tin + Tout}{2}$ (1)

Water flow rate Q = 660LPH or 11LPM

Flow rate per tube $= \frac{Q}{(2\times 76)}$ (2)

$q = 1.20614E\text{-}06\ m^3 s^{-1}$

.

Mean velocity of fluid $= \frac{q}{Ac}$ (3)

$V_w = 0.0547896\ m\ s^{-1}$

Hydraulic diameter of the tube is calculated as: (4)

$D_{hw} = \frac{4 \times Ac}{P} = 0.002776$ m

Reynolds number of the fluid is given by (5)

$R_{ew} = \frac{\rho w \times Vw \times Dhw}{\mu w}$

$R_{ew} = 131.9067$

Nusselt numbers are calculated from Shah and London's equations given as follows [20]:

$Nu_w = 4.364 + 0.0722(ReDhw\ Pr)$ (6)

$Nu_w = 4.6249$

Heat transfer coefficient is evaluated by

$h_w = \frac{Nu \times Kw}{Dhw}$ (7)

$h_w = 1145.8956\ W\ m^{-1} k^{-1}$

Friction factor $f_w = \frac{82}{Re}$ (8)

$f_w = 0.21147$

Air side or Fin Side Calculations: Aluminium-based Multi-louvered fins are provided on the air side of the radiator. These fins are attached with the radiator tubes as a functional phenomenon of conduction and convection. A control volume of the section is considered to evaluate the various parameters. Similar to the water side, Pt-100 thermocouples are pasted at different locations on air inlet (2 thermocouples) and outlet side (6 thermocouples) of the radiator. The various properties of air are taken at bulk mean temperature (sample shown in Table 6), calculated as the mean of temperature at the inlet and that at the outlet of the section. Following are the relations used to calculate the performance of the radiator at air side:

Table 6: Thermo Physical Properties of Air at Bulk Mean Temperature of 316.75K

Bulk mean temp.	Thermal conductivity (k_w), W/mK	Density (ρ_w) kg/m^3	Dynamic viscosity (μ_w) kg/m.s	Prandtl Number
316.75 K	0.02733 W/mK	1.1148 kg/m^3	1.9314E-05 kg/m.s	0.7115

Velocity of air, $V_a = 6.22\ m\ s^{-1}$

$D_{h,a}$= 7.475 E-3 m

Mass flow rate of the air = W_a kg s^{-1}

$W_a = \rho \times A_c \times V_a$ (9)

W_a = 1.1148 x 0.01976 x 6.22

W_a = 0.137016 kg s^{-1}

Heat capacity rate = W_a x $C_{p,a}$ (10)

W_a x $C_{p,a}$ =137.975

Core mass velocity = G_a

$G_a = \frac{Wa}{Ac} = 6.9340$ (11)

$R_e = \frac{Dh,a}{\mu} \times G_a$

$R_e = 2684$

Heat transfer coefficient is calculated by

$h = j_a \times G_a \times C_{pa} / (P_{ra})^{2/3}$ (12)

Where,

$j_a = (Re_{lp})^{-0.42} \times (l_h)^{0.33} \times (H_f)^{0.25} \times (L_i/h_f)^{1.1}$ (13) l_p= louver pitch l_h= louver height

l_l= louver length H_f=fin height

Reynolds Number on Louvered side = Re_{lp}

$Re_{lp} = \rho_a \times V_a \times l_p / \mu_a$ (14)

Re_{lp} = 576.33

j_a = 0.00714756

$h_a = j_a \times G_a \times C_{pa} / (P_{ra})^{2/3}$ (15)

h_a = 60.756

Fin efficiency $\eta_f = \tanh(ml)/(ml)$ (16)

where, $m = [\ 2 \times h_a / k_{fin} \times \delta]^{\ 0.5}$ (17)

η_f =0.9682

Total surface temperature effectiveness of the fin is given as:

$\eta_0 = 1.0 - (1.0 - \eta_f) \times A_f / A$ (18)

η_0 = 0.9633

Correlation to find the friction factor is given as the following:

$$fa = 0.464 \text{ x } (Re_{lp})^{0.39} \text{x } (L_h/H_f)^{0.33} \text{x } (L_i/H_f)^{1.1} \text{x } H_f^{0.46} \qquad (19)$$

$fa = 0.04702$

Heat Exchanger Effectiveness [20]

The effectiveness of the heat exchanger is calculated with the help of given relation:

heat exchanger effectiveness

$\epsilon = C_h \text{ x } (T_{h.in} - T_{h,\,out})/[\,C_{min} \text{ x } (T_{h,in} - T_{c,in})]$ (20) $\epsilon = 0.680544$

Overall Heat Transfer Coefficient

The overall heat transfer coefficient is calculated by the following relation (neglecting small resistance):

$$\frac{1}{Ua} = 1/\,\eta_0 h_a + (\frac{aw}{aa})\, h_w \qquad (21)$$

$U_a = 37.8922 \text{ Wm}^{-2} \text{ k}$

RESULTS AND DISCUSSION

Temperature-dependent rheological properties and heat-carrying characteristics of zinc oxide-based nanofluids

As mentioned earlier, various properties of nanofluids such as thermal conductivity, density and viscosity are experimentally evaluated by KD-II Pro Thermal analyzer, pycnometer and DV-1 viscometer respectively. The study has been conducted with varying temperatures and concentrations of nanofluid.

Influence of Temperature on Thermal Conductivity of the Fluid

Fig. 9 shows the influence of temperature on the thermal conductivity of ZnO nanofluid. Results reveal that the thermal conductivity of nanofluid increases with an increase in temperature. Moreover, the thermal conductivity of the nanofluids is higher than that of base fluid. The reason behind the phenomenon is only caused by the random motion of the particles within the fluid. i.e. kinetic theory of gases. This motion is only due to the collision of ZnO nanoparticles with the base fluid’s molecule. As the high-temperature particles collide with particles at low temperature, energy transfer takes place. However, an increase in the concentration of nanoparticles in fluids results in the enhancement of thermal conductivity of overall nanofluid.

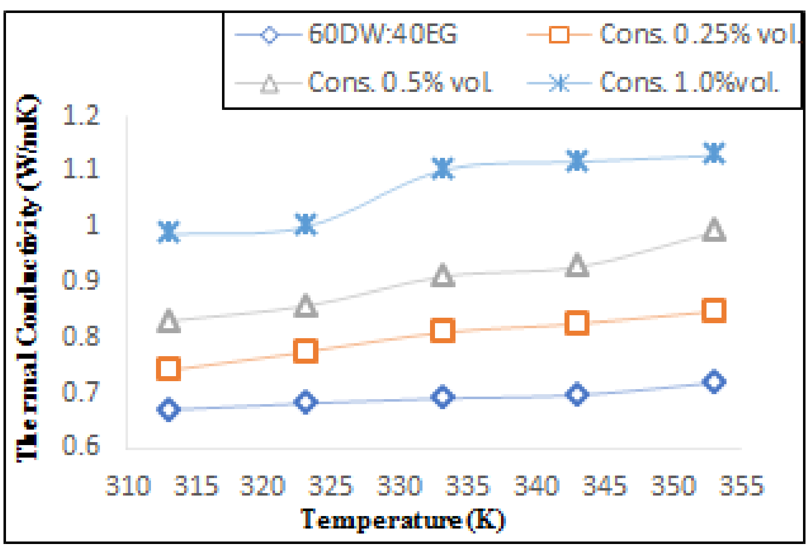

Fig. 9: Influence of Temperature on Thermal Conductivity of Fluid.

Temperature Dependence of Density Data for ZnO Nanofluid:

Fig. 10 represents the influence of temperature over the density of the nanofluid at different concentrations of zinc oxide nanoparticles. The density of the nanofluid rises to a large extent as the solid particles are added into the base fluid. The reason behind this enhancement is only due to the higher density of solid nanoparticles as compared to the density of base fluid i.e. mixture of ethylene glycol and distilled water. In addition to this, an increase in temperature leads to a slight drop in the density of the nanofluid and the same trend is followed by different concentrations of the nanoparticles into the base fluid.

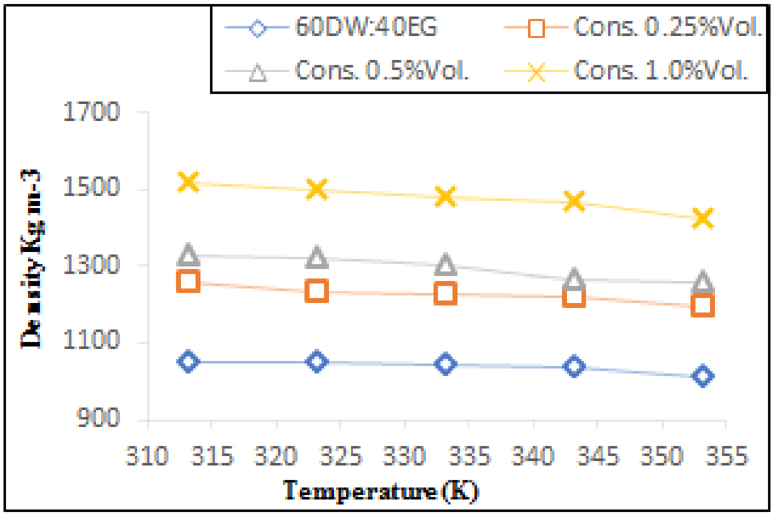

Fig. 10: Effect of Temperature on the Density at Variable Concentration

Temperature Dependence of Viscosity Data for Zinc Oxide Nanofluid

Results shown in Fig. 11 depict that the viscosity of nanofluids increases with an increase in concentration of nanoparticles into the fluid. As the solid ZnO nanoparticles are added into the base fluid, the density of the fluid increases which in turn results in preponderating of inertia forces over the viscous forces and a large amount of force is required to overcome these forces. Hence, the viscosity of the nanofluid increases. On another side, the viscosity of nanofluid decreases with increases in temperature which is caused by the loss in strength of intermolecular bonds formed by the nanofluid.

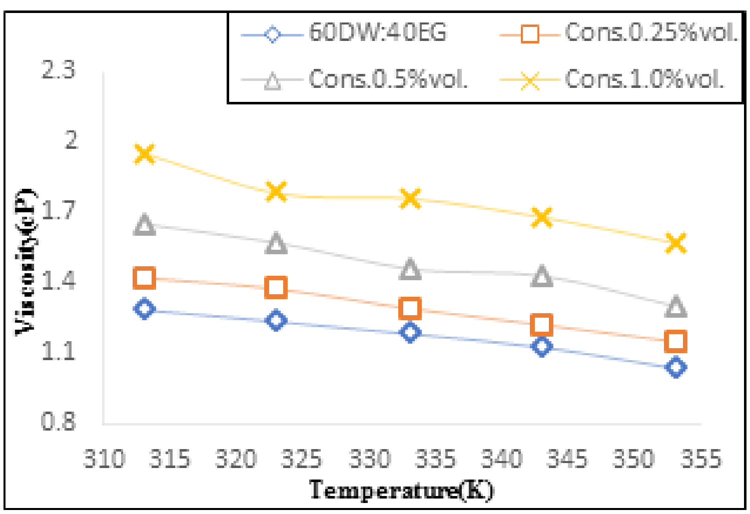

Fig. 11: Influence of Temperature and Concentration of Nanoparticles on Viscosity of Nanofluid.

Analysis for water side or tube side (hot fluid)

The experimental study has been carried out by varying the input parameters such as the inlet temperature of the fluid, concentration of nanoparticles into the fluid and flow rate of the fluid within the radiator tubes. Further tube side /water side analysis has been carried out to evaluate the heat transfer characteristics in terms of Nusselt Number and friction factor. Nusselt number is a dimensionless number that describes the temperature gradient at a surface. Additions of highly thermal conductive nanoparticles into the fluid lead to a rise in the thermal conductivity of the overall fluid which further intensifies the heat transfer rate. Moreover, the friction factor is measured to calculate the pressure drop within the radiator tubes. Heat transfer rate increases to a larger extent caused by improvement in thermal conductivity while the increase in friction factor leads to a slight increase in pumping power.

Influence of Reynolds Number and Nanofluid Concentration on Tube Side/Water Side Nusselt Number.

Results reveal as shown in Fig.12 that the Nusselt number increases with increase in Reynold number. In case of forced convection, Nusselt number is a function of Reynolds number and Prandtl number. Prandtl number depicts the properties of fluid by virtue of motion at the molecular level. However, Reynolds number represents the flow pattern i.e. laminar flow pattern and turbulent flow pattern. The major cause of increasing Nusselt numbers are the capability of suspended nanoparticles to enhance thermal conductivity and energy exchange carried by the particles at higher Reynolds number. At higher Reynolds numbers, the turbulence of fluid causes a reduction in the thickness of boundary layer which in turn results in an increase in Nusselt number.

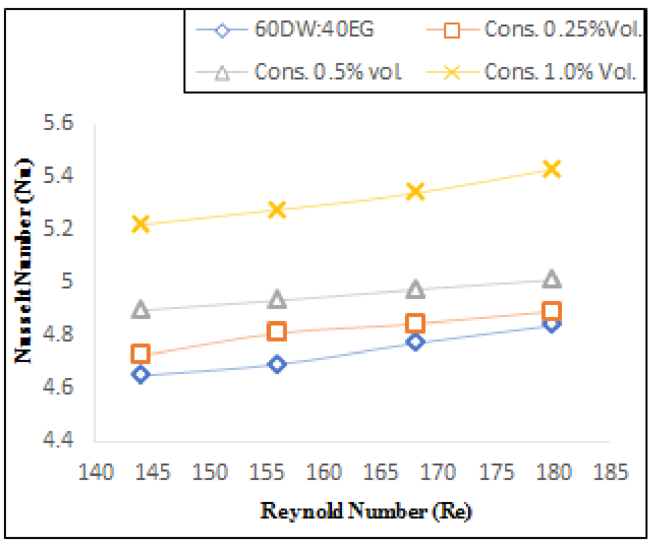

Fig. 12: Influence of Reynold Number and Nanofluid Concentration on Hot Side/Water Side Nusselt Number

Fig. 12 reveals that Nusselt number also increases with increase in concentration of particles in the fluid. The addition of solid nanoparticles into base fluid enhances inertia forces thereby causing the increase in heat transfer rate. The phenomenon behind this increment is only caused by the higher thermal conductivity and Brownian motion of the fluid. Further, an increase in concentration leads to a drop in heat transfer rate however Nusselt number increases due to the predominance behavior of thermal conductivity.

Influence of Reynold Number & Nanofluid Concentration on Friction Factor

Fig. 13 represents the effect of Reynolds number and nanofluid concentration on the friction factor. Pressure drop is measured by connecting the limbs of mercury operated U-tube differential manometer with the inlet and outlet section of the radiator and this pressure drop is further used to calculate the friction factor parameter. The result shows that when the Reynolds number starts increasing, the friction factor starts decreasing. The drop in friction factor with increase in Reynolds number is caused only by predominance of inertia forces over the viscous forces.

From the results, it is crystal clear that the addition of ZnO nanoparticles into base fluid increases heat transfer to a larger extent and friction factor to a smaller extent. Increase in friction factor represents some degree of additional pumping power to circulate the nanofluid within the radiator.

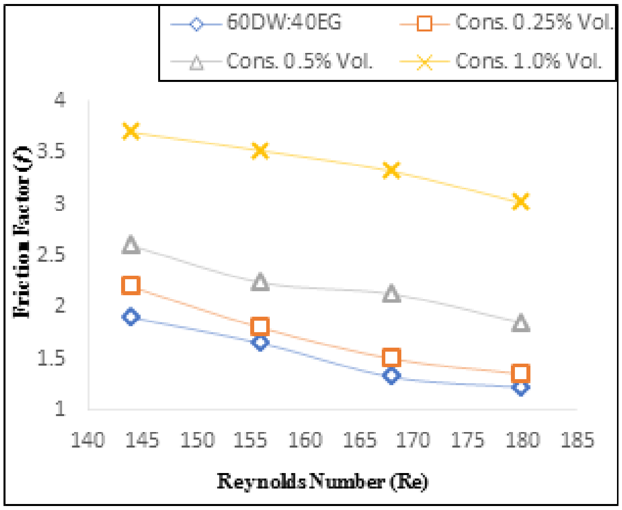

Fig. 13: Influence of Reynold Number and Nanofluid Concentration on Friction Factor

Influence of Reynold Number and Inlet Temperature of Nanofluid on Tube Side Friction Factor

Fig. 14 represents the effect of Reynolds number and inlet temperature of the nanofluids over the friction factor. As discussed earlier, increase in Reynold number results in decrease in friction factor.

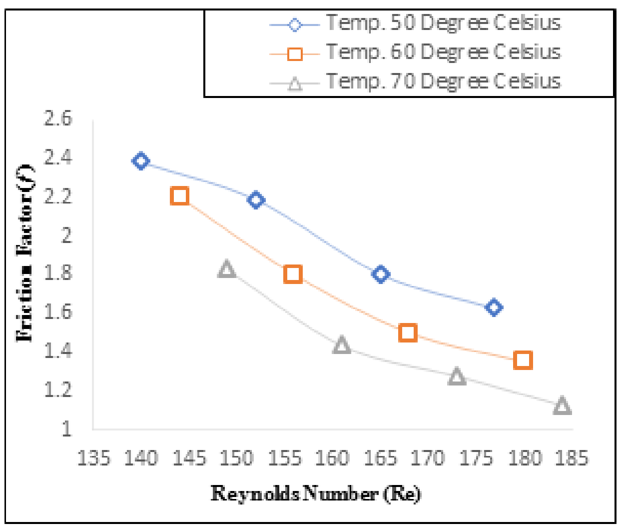

Fig. 14: Influence of Reynold Number and Inlet Temperature of Nanofluid on Tube Side Friction Factor

Moreover, increase in inlet temperature of the fluid becomes a reason for the decrease in viscosity of the nanofluid. Consequently, less amount of forces are required to overcome the inertia forces i.e. low amount of energy is needed for pumping the nanofluids. Hence, degradation in friction factor has been evaluated.

Influence of Reynolds Number and Inlet Temperature of the Nanofluids over Nusselt Number

Results as shown in Fig. 15 reveal Nusselt number increases with increase in Reynold number and inlet temperature of the nanofluid. Reynolds number is directly proportional to the density, velocity and hydraulic diameter of the radiator tube while inversely proportional to the viscosity of the fluid.

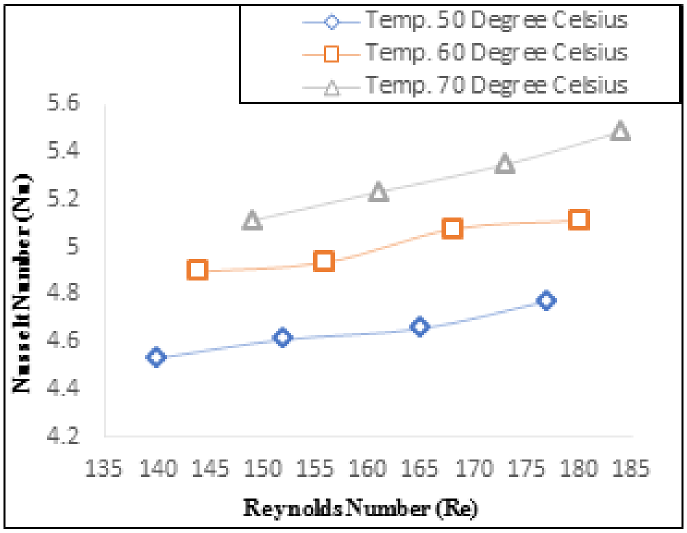

Fig. 15: Influence of Reynolds Number and Inlet Temperature of Nanofluids over the Nusselt Number

For a constant flow rate enhancement in inlet temperature leads to lower the density and viscosity of fluid. The density of nanofluid predominance over the viscosity of the nanofluid results in a high Reynolds number for higher inlet temperature. As the inlet temperature of the nanofluid rises, it helps to reduce viscosity as well as enhance the thermal conductivity of the nanofluid. Thermal conductivity of the nanofluid predominates over the viscosity and thus Nusselt number increases.

Air Side Calculation\Cold Fluid Side Analysis

For dissipating the excess amount of heat from a source, fins are employed on the surface. Fins are the extended surfaces that are generally used to enhance the heat transfer rate with the aid of increasing surface area. For the current study, Aluminium based multi-louvered fins are considered to analyze the cold side/air side performance of heat exchanger. For air side analysis of heat exchanger, the friction that occurs when the cold air passes through the fins to dissipate the heat and the fin's geometry are taken into account. Moreover, the Nusselt number, friction factor and Colburn factor are considered to analyze the thermal performance of a multi-louvered cross-flow heat exchanger.

Effects of Reynolds Number and Nanofluids Concentration on Air Side Nusselt Number

Fig. 16 represents the influence of air Reynolds number and nanofluid concentration on the air side Nusselt number. In contrast, the amount of enhancement in heat transfer rate is directly proportional to the motion of fluid which is further dependent on the thickness of the boundary layer with respect to the existence of temperature gradient. Implementation of multi-louvered fins are major reason for enhancement in heat transfer rate as it permits to dissipate the huge amount of heat by smashing the boundary layer thickness. Thus, an increase in Nusselt number has been evaluated at a higher degree of Reynolds number. On another side, the addition of ZnO nanoparticles into the fluid raised the thermal conductivity of overall fluid resulting in increase in Nusselt number which further leads to increase in the heat transfer rate.

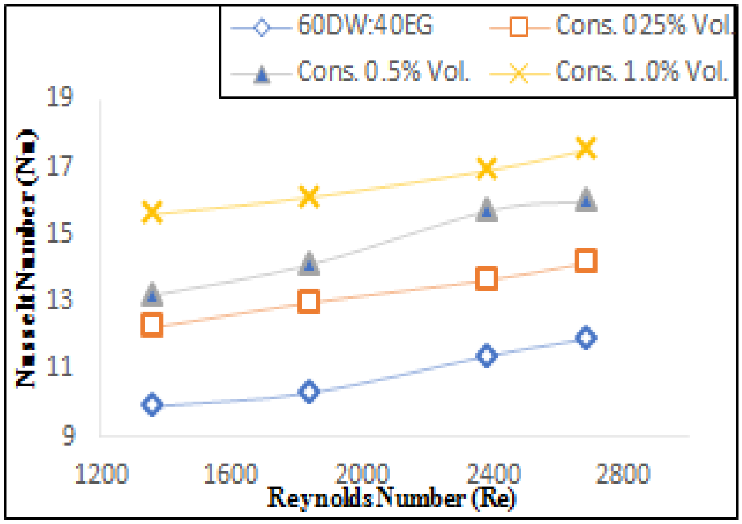

Fig. 16: Influence of Air Reynolds Number and Nanofluids Concentration on Air Side Nusselt Number

Influence of Air Reynolds Number and Nanofluids Conc. on Air Side Friction Factor

Fig. 17 shows the influence of air side Reynold number and water side fluid concentration on the friction factor. In a deep glance, it is observed that the friction factor is inversely proportional to the air side Reynold number and directly proportional to the nanofluid.

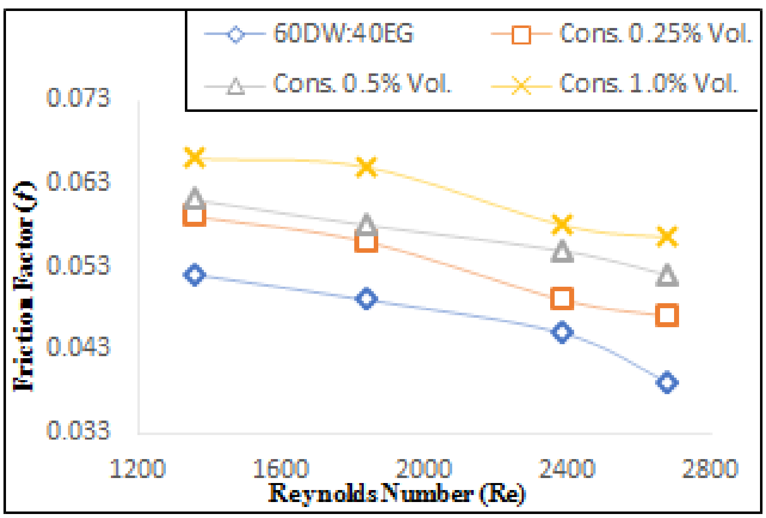

Fig. 17: Influence of Air Reynolds Number and Nanofluids Concentration on Air Side Friction Factor

As discussed earlier, fins are the extended surfaces implemented to eliminate the excess amount of heat from heat-carrying resources by virtue of generating friction between cold fluid (air) and multi-louvered surfaces. This, in turn, enhances the heat transfer rate with a slight increase in pressure drop. Enhancement in Reynolds number leads to deformation of the boundary layer formed over the extended surfaces and less quantity of drag forces are required to break the thermal boundary thus friction factor starts decreasing. However, enhancement in thermal conductivity is caused by the increase in nanofluid concentration i.e. huge amount of heat transfer to fins. Hence, cold fluid is required to break the thick layer of the thermal boundary. As a result, an increment has been found in the friction factor at higher concentrations of nanoparticles in the base fluid.

Effect of Reynolds Number and Inlet Fluid Temperature of Fluid on Air Side Nusselt Number

Fig. 18 represents the influence of Reynold number and inlet fluid temperature on the air side Nusselt number. It is found that Nusselt numbers increase with the increase in Reynold number of air. Reynolds number and Prandtl numbers are coefficients of Nusselt number (dimensionless number, heat transfer) which represent the temperature gradient at a surface. As the temperature of inlet fluid that flow within the radiator tubes rises, the surface temperature of the heat exchanger increases. This enhancement has the capability to alter the rheological properties such as density and viscosity of the cold fluid (air). The density of the air decreases to some extent while viscosity increases at a higher rate and this enhancement becomes a reason for the increase in Nusselt number.

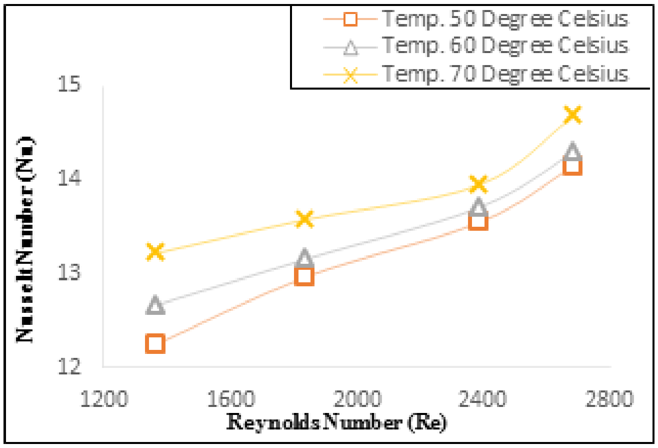

Fig. 18: Effect of Reynolds Number and Inlet Fluid Temperature of Fluid on Air Side Nusselt Number

Influence of Reynold Number and Inlet Fluid Temperature on Air Side Friction Factor

Fig. 19 depicts the effect of Reynolds number and inlet temperature of the fluid on air side friction factor.

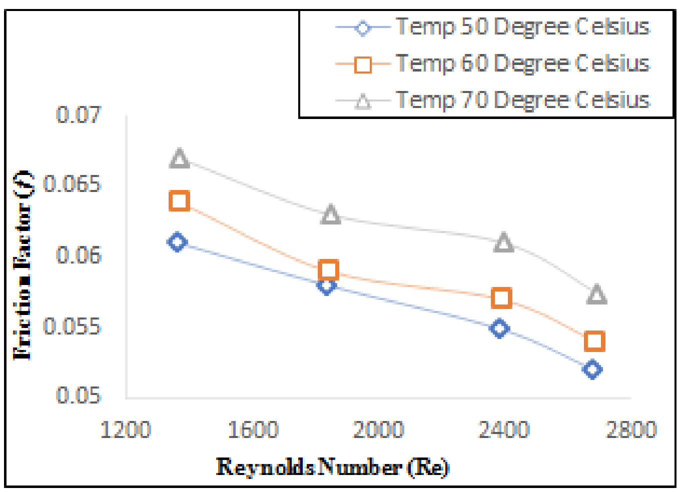

Fig. 19: Influence of Reynold Number and Inlet Fluid Temperature on Air Side Friction Factor.

At the initial stage, for 50^{O}C inlet temperature friction factor stood at topmost position and continuously dropped with the rise in Reynolds number. A similar trend has been found for 60^{O}C and 70^{O}C inlet temperature. On the other hand, increase in the inlet temperature of the nanofluid raises the surface temperature of the heat exchanger. Consequently, the surface temperature of the extended surfaces i.e. multi-louvered fins increases which causes more amount of friction between the fins and cold fluid (Air) passing over the fins and results in a high friction factor at high inlet temperature of nanofluid.

Influence of Reynolds Number and Nanofluid Conc. on Colburn Factor of the Air

Fig. 20 represents the influence of Reynolds number and nanofluid concentration on the Colburn factor of the air at 60^{O}C inlet temperature of fluid. Results depict that the Colburn factor of air increases with increase in particle volume concentration and decreases with increase in Reynolds number of air. The Colburn factor is a dimensionless heat transfer coefficient used to calculate the heat transfer rate over a flat surface. The Colburn factor is a function of Stanton number and Prandtl number and is taken into consideration for the analysis of heat transfer characteristics at the air side/ fin side of the radiator [21].

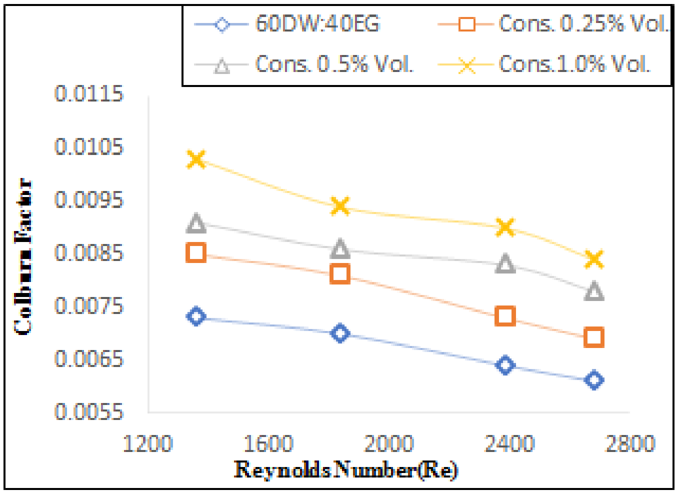

Fig. 20: Influence of Reynolds Number and Nanofluid Concentration on Colburn Factor of the Air

Results show that for drops in heat transfer coefficient of cooling fluid, the Stanton number decreases. Consequently, the Colburn factor of air decreases.

Thermo Hydraulic Performance of Aluminium-based Multi-louvered Fin Operated Cross Flow Heat Exchanger

The experiment is conducted to analyze the thermo-hydraulic performance of a multi-louvered fin-operated car radiator with the aid of conventional fluid and ZnO nanofluid and thereafter comparisons have been made. The effectiveness of the heat exchanger is analyzed at bulk mean temperature. Experimental result depicts that the effectiveness of heat exchanger significantly upgrades with the use of water and ethylene glycol-based Zinc oxide nanofluid. It is calculated as 66.54% for base fluid (mixture of distilled water and ethylene glycol) and enhanced to 68.05%, 71.88% and 75.29 % for 0.25, 0.5 and 1.0% of volumetric concentrations respectively.

Further overall heat transfer coefficient has been evaluated by the rate of heat transfer, the geometry of fins and log mean temperature difference which is enhanced by 19.87%, 22.04% and 25.33% for 0.25%, 0.5% and 1.0% volumetric concentration as compared to base fluid.

CONCLUSIONS

The experiment was conducted on an Al-based multi-louvered fin car radiator by developing the experimental test rig. Various input parameters that influence thermo hydraulic performance of heat exchanger (radiator) such as coolant flow rate(12,13,14 and 15LPM), inlet temperate of coolant (50,60 and 70 ^{O}C) and velocity of cooling air (3.16, 4.26,5.53 and 6.22 m/s) were analyzed for both conventional fluid (mixture of distilled water and ethylene glycol) as well as ZnO based nanofluid (0.25%,0.5% and1.0% volumetric concentration) and thereafter comparison has been made. The following conclusions are drawn based on experimental study:

Rheological Properties of Zinc Oxide-based Nanofluid:

- Thermal conductivity is found to be a strong function of temperature. For base fluid, increments of 7.462% in thermal conductivity were observed as the temperature rose from 313.15 K to 353.15K. In addition, within a similar temperature range 14.285%, 19.374% and 13.96% enhancement in thermal conductivity have been observed with 0.25%,0.5% and 1.0% volumetric concentration respectively.

- As the solid nanoparticles of Zinc oxide are added into the base fluid, the density of the nanofluid increases slightly. However, a drop-in density has been observed when the temperature of the nanofluid increases. Enhancement by 05.489% in density is recorded when the volumetric concentration of nanofluid increases from 0.25% to 0.5%. However, a noticeable drop in density has been recorded by 3.992%, 4.773%, 5.354% and 6.389% for base fluid, 0.25%,0.5% and 1.0% volumetric concentration respectively when the temperature increases from 313.15 K to 353.15 K.
- Although the viscosity of nanofluid is slightly higher as compared to the base fluid but it decreases with an increase in temperature. Among all concentrations, a maximum drop in viscosity by 21.173% has been found for 0.5% volumetric concentration as the temperature rises from 313.15 K to 353.15K.

Tube Side / Water Side Execution of Heat Exchanger

- Enhancement in Reynold number and volumetric concentration of nanofluid results in enhancement in Nusselt number. Consequently, heat transfer rate hikes. At a flow rate of 14 LPM i.e. Reynolds number 168 (approx.), Nusselt numbers are enhanced by 1.548%,4.262% and 11.92% for 0.25%, 0.5% and 1.0% volumetric concentration as compared to that of the base fluid.
- Nusselt number of nanofluid increases with increase in inlet temperature. At a certain concentration of nanofluid, a noticeable enhancement by 7.987% and 12.797% has been observed when the inlet temperature of nanofluid rises by 10 K and 20 K respectively as compared to base temperature.
- Friction factor increases with increase in nanofluid concentrations. For 333.15K inlet temperature, friction factor drops by 35.578%, 38.636%, 29.916% and 12.069% for base fluid, 0.25%, 0.5% and 1.0% volumetric concentration as the Reynolds number raises from 144 to 180. At 1.0% volumetric concentration of nanofluid, a maximum enhancement of 52.631% has been noticed in friction factor when compared to that of the base fluid.
- Friction factor decreases with increase in inlet temperature of the nanofluid. When the inlet temperature is enhanced to 333.15K and 343.15K, for 0.25% volumetric concentration, the friction factor drops by 23.319% and 7.563%with respect to 323.15K.
- On the tube side/water side, a significant hike by 18.741%, 22.351% and 26.464% has been observed in heat transfer coefficient for 0.25%, 0.5% and 1.0% volumetric concentration with respect to the base fluid.

Fin Side /Air Side Execution of Heat Exchanger

- Enhancement of Nusselt numbers has been observed as the Reynolds number increases. Average Nusselt increases by 21.88%, 35.58% and 51.91% with 0.25%, 0.5% and 1.0% volumetric concentration respectively as compared to that of the base fluid.
- Nusselt number for air increases with an increase in Reynolds number of cooling fluid (Air). For 0.5% volumetric concentration, 15.510% enhancement in Nusselt number is observed at 323.15K inlet temperature of the fluid while it is recorded as 12.786% and 11.043% for 333.15K and 343.15K respectively.
- Friction factor decreases with increase in air Reynolds number and increases with increase in nanofluid concentration. For a certain inlet temperature, enhancement in friction factor by 13.46%,17.30% and 26.92% has been observed for 0.25%, 0.5% and 1.0% concentration of nanofluid respectively in concern with base fluid.
- For 0.5% nanoparticle volume concentration, the friction factor of air is increased by 4.754% and 9.836% at 333.15K and 343.15K respectively with respect to inlet temperature of 323.15K.

- As compared to base fluid as a coolant, the Colburn factor of air is enhanced by 16.439%, 24.657% and 41.096% for 0.25%, 0.5% and 1.0% concentration of nanofluid.

Overall Performance of Heat Exchanger

- The effectiveness of the heat exchanger is analyzed by comparing the performance of nanofluid when circulating into the radiator tubes at different concentrations and with the base fluid at similar boundary conditions. Consequently, it is found that the effectiveness of the heat exchanger is calculated as 66.54% for base fluid (mixture of distilled water and ethylene glycol) and enhanced to 68.05%, 71.88% and 75.29 % for 0.25, 0.5 and 1.0% of volumetric concentrations respectively.
- Further, the overall heat transfer coefficient has been evaluated by rate of heat transfer, the geometry of fins and with log mean temperature difference which is enhanced by 19.87%, 22.04% and 25.33% for 0.25%, 0.5% and 1.0% volumetric concentration as compared to that of base fluid.

REFERENCES

[1] Esfe, M.H., Saedodin, S. and Mahmoodi, M., 2014. Experimental studies on the convective heat transfer performance and thermophysical properties of MgO–water nanofluid under turbulent flow. *Experimental thermal and fluid science*, *52*, pp.68-78.

[2] Madhesh, D., Parameshwaran, R. and Kalaiselvam, S., 2014. Experimental investigation on convective heat transfer and rheological characteristics of Cu–TiO2 hybrid nanofluids. *Experimental Thermal and Fluid Science*, *52*, pp.104-115.

[3] Choi, S.U. and Eastman, J.A., 1995. *Enhancing thermal conductivity of fluids with nanoparticles* (No. ANL/MSD/CP-84938; CONF-951135-29). Argonne National Lab.(ANL), Argonne, IL (United States).

[4] Eastman, J.A., Choi, S.U.S., Li, S., Yu, W. and Thompson, L.J., 2001. Anomalously increased effective thermal conductivities of ethylene glycol-based nanofluids containing copper nanoparticles. *Applied physics letters*, *78*(6), pp.718-720.

[5] Masuda, H., Ebata, A. and Teramae, K., 1993. Alteration of thermal conductivity and viscosity of liquid by dispersing ultra-fine particles. Dispersion of Al2O3, SiO2 and TiO2 ultra-fine particles.

[6] Lee, S., Choi, S.S., Li, S.A. and Eastman, J.A., 1999. Measuring thermal conductivity of fluids containing oxide nanoparticles.

[7] Leong, K.Y., Saidur, R., Kazi, S.N. and Mamun, A.H., 2010. Performance investigation of an automotive car radiator operated with nanofluid-based coolants (nanofluid as a coolant in a radiator). *Applied Thermal Engineering*, *30*(17-18), pp.2685-2692.

[8] Kalantari, D., Tafakhori, M., Ghanbari, M., Biparva, P. and Peyghambarzadeh, S.M., 2023. Intensification of thermal efficiency of a cross-flow heat exchanger under turbulent flow conditions using CuFe2O4/water nanofluid. *International Journal of Thermal Sciences*, *185*, p.108107.

[9] Ahmed, S.A., Ozkaymak, M., Sözen, A., Menlik, T. and Fahed, A., 2018. Improving car radiator performance by using TiO2-water nanofluid. *Engineering science and technology, an international journal*, *21*(5), pp.996-1005.

[10] Li, X., Wang, H. and Luo, B., 2021. The thermophysical properties and enhanced heat transfer performance of SiC-MWCNTs hybrid nanofluids for car radiator system. *Colloids and Surfaces A: Physicochemical and Engineering Aspects*, *612*, p.125968.

[11] Hafeez, M.B., Amin, R., Nisar, K.S., Jamshed, W., Abdel-Aty, A.H. and Khashan, M.M., 2021. Heat transfer enhancement through nanofluids with applications in automobile radiator. *Case Studies in Thermal Engineering*, *27*, p.101192.

[12] Kalantari, D., Tafakhori, M., Ghanbari, M., Biparva, P. and Peyghambarzadeh, S.M., 2023. Intensification of thermal efficiency of a cross-flow heat exchanger under turbulent flow conditions using CuFe2O4/water nanofluid. *International Journal of Thermal Sciences*, *185*, p.108107.

[13] Said, Z., Assad, M.E.H., Hachicha, A.A., Bellos, E., Abdelkareem, M.A., Alazaizeh, D.Z. and Yousef, B.A., 2019. Enhancing the performance of automotive radiators using nanofluids. *Renewable and Sustainable Energy Reviews*, *112*, pp.183-194.

[14] Goudarzi, K. and Jamali, H., 2017. Heat transfer enhancement of Al2O3-EG nanofluid in a car radiator with wire coil inserts. *Applied Thermal Engineering*, *118*, pp.510-517..

[15] Ma, B. and Banerjee, D., 2018. A review of nanofluid synthesis. *Advances in Nanomaterials: Fundamentals, Properties and Applications*, pp.135-176.

[16] Gangacharyulu D, Sharma S, Kumar S. some studies of heat transfer and pressure drop characteristic of CuO-distilled water based nanofluid. M. Tech. Dissertation.T. U., Patiala

[17] Brookfield Digital Viscometer, Model DV-E, Operating Instructions, Manual No. M/98-350-g0307, Brookfield Engineering Laboratories, Inc., 11 Commerce Boulevard, Middleboro, MA 02346 USA.

[18] Gangacharyulu D, Sharma JK, Singh G. Performance evaluation of after cooler in diesel engines—a case study. IE(I) 1999;19(6):625–39.

[19] Bohne, D., Fischer, S. and Obermeier, E., 1984. Thermal, conductivity, density, viscosity, and Prandtl-numbers of ethylene glycol-water mixtures. *Berichte der Bunsengesellschaft für physikalische Chemie*, *88*(8), pp.739-742.

[20] Shah, R.K. and London, A.L., 2014. *Laminar flow forced convection in ducts: a source book for compact heat exchanger analytical data*. Academic press.

[21] Li, W. and Wang, X., 2010. Heat transfer and pressure drop correlations for compact heat exchangers with multi-region louver fins. *International Journal of heat and mass transfer*, *53*(15-16), pp.2955-2962.